doi:

A. GORIACHKO,[1] P.V. MELNIK,[1] M.G. NAKHODKIN[2]

[1] Department of Physical Electronics,
Taras Shevchenko National University of Kyiv
(4G, Academician Glushkov Ave., Kyiv 03022, Ukraine; e-mail: andreandy2000@gmail.com)
[2] Department of Nanophysics and Nanoelectronics,
Taras Shevchenko National University of Kyiv
(4G, Academician Glushkov Ave., Kyiv 03022, Ukraine)

A SUGGESTION OF THE GRAPHENE/Ge(111) STRUCTURE BASED ON ULTRA-HIGH VACUUM SCANNING TUNNELING MICROSCOPY INVESTIGATION

PACS 61.72.uf, 68.35.B-, 68.37.Ef

We report on the $5.5\sqrt{3} \times 5.5\sqrt{3} - R30^\circ$ overlayer superstructure observed by the scanning tunneling microscopy on the Ge(111) surface. It shows pronounced effects of the local density of states leading to the strong dependence of STM images on the bias voltage and some dynamic changes of images at 300 K. This overlayer is tentatively interpreted as graphene formed in small submonolayer amounts due to the pyrolysis of hydrocarbon constituents of the residual atmosphere of the vacuum chamber during the annealing of a Ge(111) sample at 900 K. We suggest a model of the graphene/Ge(111)-$5.5\sqrt{3} \times 5.5\sqrt{3} - R30^\circ$ heteroepitaxial interface, featuring the reconstructed Ge(111) substrate with no long-range order under the graphene layer, the latter being corrugated due to spatial variations of the interatomic geometry of the Ge(111) and graphene(0001) atomic lattices with extremely large mismatch.

Keywords: germanium, graphene, scanning tunneling microscopy.

1. Introduction

The first isolation of graphene (g-C) on the SiO_2 substrate by A.K. Geim and co-workers [1] had led to the emergence of the physics of graphene and other two-dimensional crystals. Due to its truly fascinating and unique physical properties [2], graphene was widely studied on various substrates, as dictated by a myriad of possible practical applications. The range of substrates includes metals, as reviewed in [3], the wide-band-gap semiconductor SiC [4], and insulators [5]. At the same time, there are no studies of graphene on a substrate made of a semiconductor, although such combination may be of interest from the purely scientific or practical point of view. In particular, in view of the high electrical conductivity and astonishing optical transparency of g-C [6], it can serve as a perspective optoelectronic material or can be an important interface between the traditional microelectronics and a novel graphene-based two-dimensional nanoelectronic circuitry [7].

For a heteroepitaxial graphene film, the possible semiconductor substrates with a moderate band gap are, first of all, silicon and germanium. The former is severely handicapped due to a full solubility of carbon in silicon, which manifests itself by the existence of a stable SiC compound. Because of this, any deposition of carbon accompanied by elevated temperatures will tend to produce SiC at and below sample's surface [8], instead of the atomically sharp C/Si interface. This difficulty may impede any attempt to deposit graphene on Si by means of the chemical vapor deposition (CVD) technique, as widely used on metallic substrates via various hydrocarbon precursors [9]. The CVD is likely the most feasible technique for a large-scale graphene production, but requires high temperatures of the substrate to crack the precursor molecules and form the desired graphene layer. The remaining possibility to attain a true g-C/silicon interface would be a mechanical transfer of graphene onto Si(111)-7×7 in the ultra-high vacuum (UHV) environment, the latter being an absolute requirement to sustain an atomically clean silicon surface. Effectively, this can be a UHV-remake of the al-

ready well-known original procedure of obtaining g-C on silicon dioxide wafers [10]. There are too many expenses and technical complications along this route, effectively deterring experimentalists from considering the g-C/Si interface.

Germanium has an advantage of the negligible solid phase solubility of carbon in it [11], while the Ge(111) surface is expected to be the best choice for a high-quality heteroepitaxial graphene film from the symmetry viewpoint, similar to numerous cases of (111) metal substrates [3]. A surprisingly little attention has been paid to the C/Ge(111) system so far. An early investigation of the C adsorbate in the submonolayer coverage range (0.12 ML) has elucidated a $\sqrt{3} \times \sqrt{3}$ superstructure on the top of Ge(111) by means of the low-energy electron diffraction [12]. Recently, the successful deposition of graphene on the germanium substrate by means of the ambient-pressure CVD (APCVD) was reported [13], although no details of the substrate orientation and the state of its surface were provided. The obtained g-C/Ge sample was investigated by means of Raman spectroscopy and electron diffraction, thus lacking any microscopic insight. This warrants a further study of the C/Ge(111) system by means of UHV scanning tunneling microscopy (STM), while the UHV conditions should allow one to prepare a well-defined (atomically clean and reconstructed) Ge substrate.

2. Experimental

The preparation of samples and its investigation were performed entirely in a UHV chamber (the base pressure is 2×10^{-10} mbar), which is a precondition for obtaining an atomically clean and smooth germanium surface. A Ge(111) wafer (microelectronics grade surface finish, *p*-type, Ga-doped, 0.3 Ohm $\cdot$ cm) was prepared by several interchanged cycles of bombardment by Ar^+ ions (0.5 keV) at 300 K and the annealing at 900 K. The latter was achieved by the electron bombardment of the rear side of the sample. After the final annealing step, the annealing power was reduced to zero for 10 minutes, while the cooling down to room temperature by the natural heat dissipation was lasting for several more hours. The Ge(111) sample prepared according to the procedure outlined above has an atomically clean reconstructed surface.

The STM imaging was performed at room temperature (in order to avoid any excessive thermal drift) in the constant-current mode using an original home-made microscope [14]. Probe tips were made of platinum-iridium wire (80% Pt, 20% Ir) by means of the simple mechanical cutting, followed by the conditioning procedure in UHV, which was previously developed in our laboratory [15]. Images of the sample, which were prepared according to the procedure outlined above, revealed a predominant Ge(111)-c(2×8) reconstruction with some inclusions of the c(2×4) and 2×2 reconstructed areas in full agreement with our previous works [16–18] and the works of other authors [19–22]. They were used for the lateral and vertical calibrations of our STM measurement setup with the 0.8 nm $\times$ 3.2 nm size of a c(2×8) unit cell and a 0.33-nm single atomic step height on the reconstructed Ge(111) surface.

The Auger electron spectroscopy (AES) was utilized for the elemental analysis of sample's surface by means of the excitation by 3-keV primary electrons and gathering the data with the help of a cylindrical mirror energy analyzer coupled to a secondary electron multiplier as a signal detector. AES spectra were registered in the differential EdN/dE mode.

Even if an atomically clean substrate is being held under the UHV conditions, it is slowly gathering contaminations (primarily hydrocarbon molecules from the residual atmosphere of a vacuum chamber). Typically in approximately one day, these contaminating adsorbates were hindering the stable STM imaging by introducing instabilities into the tunneling junction between the atomically clean sample and the probe tip. In order to alleviate this problem, the full surface preparation (ion bombardment and annealing) could be repeated, or, alternatively, the sample could only be annealed at 900 K. In the latter case, a small fraction of the surface area was covered by an overlayer of the previously unidentified surface superstructure, while the majority of locations were again the adsorbate-free and atomically clean reconstructed Ge(111) surface.

3. 2D Overlayer on Ge(111)

The sputtering and annealing cycles specified above yielded a reconstructed Ge(111) with atomicaly flat terraces "t" more than 100 nm in width, separated by single atomic steps "s" (Fig. 1, *a*). Here, the lateral scope is too large for any atomic details to be visible. If the regular Ge(111)-c(2×8) surface was left for an extended period of time (one or two days) in our UHV chamber and then "refreshed" afterward by

the annealing for several minutes at 900 K, than the appearance of the minority of surface locations has changed dramatically (Fig. 1, *b*). In the given case, a two-dimensional (hence, designated as 2D) hexagonal superlattice is clearly visible on the left-most terrace on the 125 nm × 125 nm scale. In what follows, it will be referred as a 2D overlayer or superlattice. As a guide for an eye, this superlattice is outlined by the black mesh in the upper left corner and is shown on the 25 nm × 25 nm inset in detail. It is important to realize that the periodicity of 2D overlayer's rippling is roughly an order of magnitude larger than a typical atomic corrugation on the pure Ge(111) substrate.

Next, we obtained the STM images in the atomic resolution (25 nm × 25 nm field of view) in order to reveal further details of various superstructures on our sample. Figure 2, *a* shows a representative area of the pure germanium surface with two atomically flat terraces separated by a single atomic step "s". The Ge(111) reconstructions are visible on the terraces: the c(2 × 8), which is the ground state of the ideal Ge(111) in UHV (unit cell outlined in white), and related less stable structures originating from defects: c(2 × 4) – outlined in black and 2 × 2 – outlined in white. The cross-section taken along the black dashed line is presented in the right-most part of Fig. 2 and shows an atomic corrugation of the outermost layer of Ge atoms on the top of the terraces, as well as the step edge between the upper and the lower terrraces.

Figure 2, *b* is a representative area with partial coverage by the 2D overlayer of the same type as observed in Fig. 1, *b*. Here, the pure Ge surface (albeit extremely large number of defects) is sandwiched between two overlayer fragments (marked by 2D) in the upper right and lower left corners. The periodic superlattice corrugation is outlined by the mesh superimposed on the upper right part of Fig. 2, *b*. The cross-section taken along the white dashed line is given to the right of the STM image and shows a ca. 0.3 nm step height between the pure Ge substrate and the 2D overlayer. Such step height strongly hints on the single atomic thickness of this yet unidentified overlayer, which is just slightly below the 0.33-nm single atomic step height between two neighboring pure Ge terraces on the Ge(111) sample.

We can estimate the most important parameters of the periodic large scale corrugation of the 2D superlattice observed on the selected areas of our sample. This corrugation is essentially a hexagonal array of height (brightness) maxima with unit vectors rotated by 30° relative to the unit vectors of 2 × 2 and c(2×8) superstructures or, equivalently, relative to in-plane unit vectors of the intrinsic Ge(111). From the cross-section *b*, the magnitude of height corrugation is up to 0.1 nm, which is well below the single atomic step height between two neighboring pure Ge terraces on the cross-section *a*. The lateral periodicity of the height maxima placement is ca. 3.8 nm, which is an order of magnitude higher than a typical in-plane interatomic separation, as exemplified by the corrugation on atomically flat terraces in cross-section *a*. However, in panel 2, *b*, one cannot but notice some irregularity of the shape and the exact placement of brightness maxima within the 2D superlattice, which

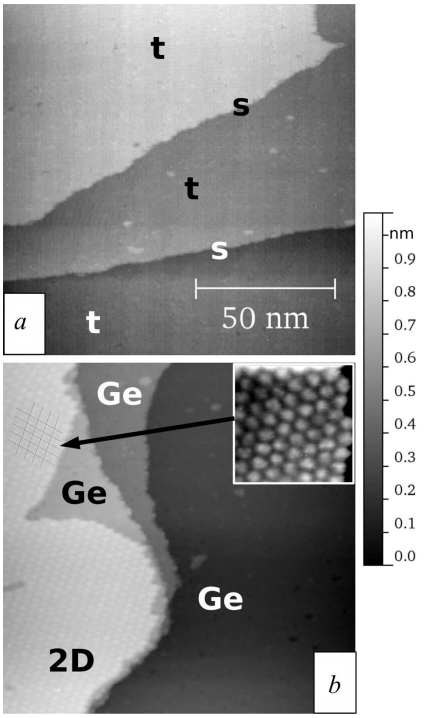

Fig. 1. Large scale STM images (125 nm × 125 nm field of view) of the Ge(111) sample: a representative area after the standard preparation procedure (*a*); specially selected area after the standard preparation followed by a prolonged stay in UHV and one more additional annealing cycle at 900 K (*b*). The black mesh and the 25 nm × 25 nm inset outline a newly observed 2D hexagonal superstructure. The grey scale to a height conversion ruler on the right side is common for both images. Sample bias voltage: +2 V; tunneling current: 0.3 nA

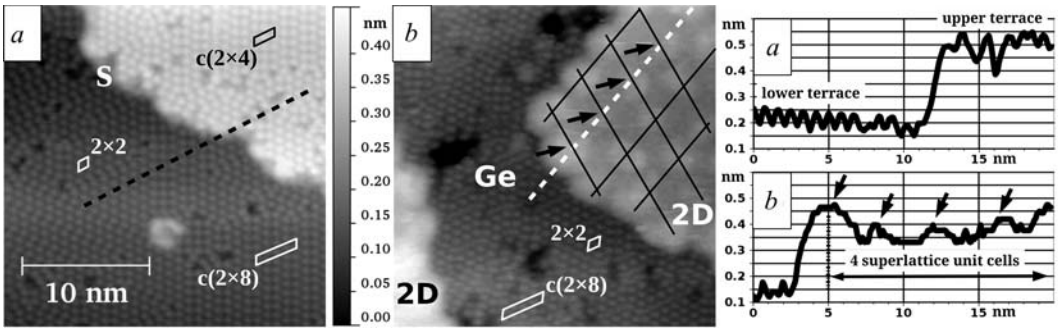

Fig. 2. STM images in atomic resolution (25 nm × 25 nm field of view) of: pure reconstructed Ge(111) surface, sample bias voltage: +2.5 V; tunneling current: 0.3 nA. c(2 × 8), c(2 × 4) and 2 × 2 superstructures are present, their unit cells are outlined and marked, correspondingly; a single atomic step between the upper and lower neighboring terraces is designated by "S" *a*. The mixture of pure Ge and a 2D hexagonal overlayer, sample bias voltage: +2 V; tunneling current: 0.3 nA, outlined are the 2 × 2 and c(2 × 8) unit cells on the pure Ge area and the 2D superlattice formed by height maxima (black mesh). On the right are height-distance cross-sections along dashed lines in corresponding panels. The height maxima lying along the cross-section line are designated by small black arrows *b*. The grey scale to a height conversion ruler is common for both images

could pose a problem for the precise determination of corrugation's magnitude and periodicity.

4. Voltage-Dependent STM of the 2D Overlayer

In what follows, we investigate a homogeneous area of the 2D overlayer on our sample. Different panels of Fig. 3 show the same area on the sample excluding some shifts due to the residual thermal drift and piezoscanner's creep. In Fig. 3, *a*, the corresponding superstructure is imaged in empty states at +3 V sample bias voltage. Under the given tunneling conditions, the superstructure looks similar to one observed in Figs. 1, *b* and 2, *b*. Namely, it exhibits a 2D periodic hexagonal corrugation with ca. 3.8 nm lateral period and magnitude below 0.1 nm.

The irregular nature of the superlattice, which was already noticeable in Fig. 2, *b* is highlighted by STM images at lower bias voltages, as demonstrated by Fig. 3, *b*–*e*. In panel 3, *b* at +2.5 V, each superlattice corrugation maximum splits into several small bright objects of the atomic size. Their number, shape, and placement within the area nominally occupied by a single superlattice site appear to be random (as demonstrated by cross-sections *c1*, *f1* and *h1*). In particular, there are superlattice sites with only one such bright object or completely without them (the latter case is marked on cross-section *f1*). It is worth to note that the transition between the types of topography, as between panels 3, *a* and 3, *b*, could also be observed at lower sample bias voltages depending on the STM probe tip condition (i.e. not necessarily between +3 V and +2.5 V).

A further lowering of the positive bias voltage magnitude to +2 V in Fig. 3, *c* and to +1.5 V in Fig. 3, *d* produces images with shape and placement of the small bright objects different from each other and those in Fig. 3, *b*. In Figs. 3, *b*–*d*, some periodic lattice on the atomic scale is clearly discernible at the locations of superlattice height minima (one such region is outlined at cross-section *c1*). This atomic lattice doesn't appear to possess a long-range order, but shows a local periodicity rather close to 0.8 nm, which, along with its symmetry, is strongly suggestive of the 2 × 2 reconstruction on Ge(111). In panel 3, *e* at +1 V, the various atomic-scale details in the STM image are rather irregular, although their brightness distribution still bears some traces of the superlattice. Due to the short tip-sample distance, a substantial scratching of the tip vs the surface has occurred during the scanning at +1 V for the given probe tip configuration.

At negative bias voltages of –2.5 V in Fig. 3, *f* and –2 V in Fig. 3, *g*, the small bright objects are also present, but they are sharper and of higher contrast relative to the superlattice corrugation. Their exact shape and placement around the superlattice sites are different in panels 3, *f* and 3, *g*. They do not coincide also with any of those obtained at positive bias voltages (panels 3, *b*–*d*). The periodic atomic lattice between the superlattice sites is barely visible at negative bias voltages both in Figs. 3, *f* and 3, *g*. Sur-

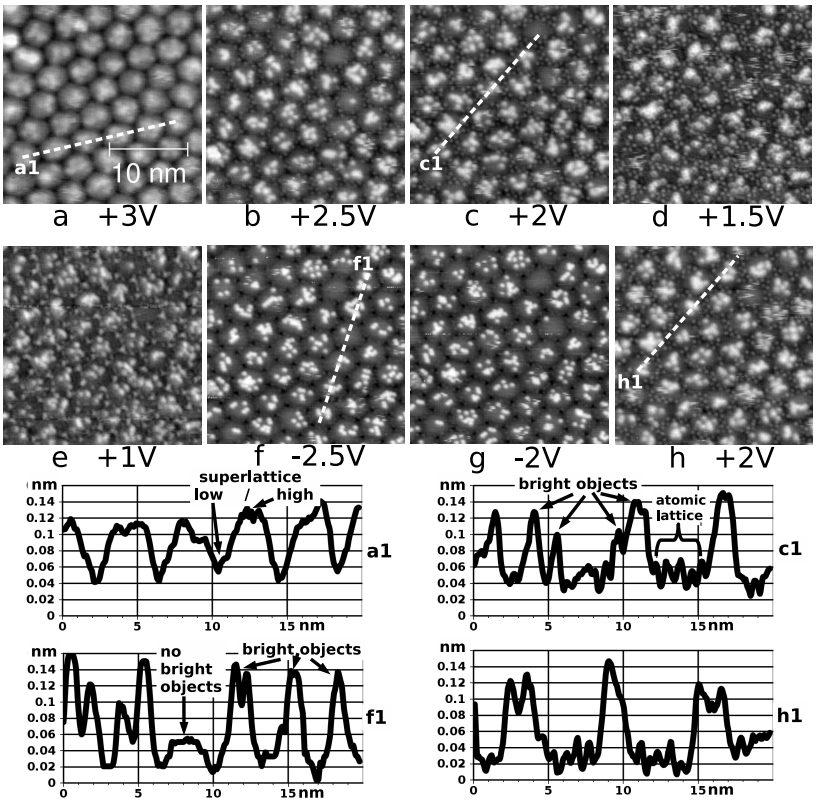

Fig. 3. STM images of the 2D overlayer superlattice at various bias voltages. All images are 25 nm × 25 nm in size and show the same area on the sample, except for some shifts due to thermal drift and creep. Sample bias voltages are: +3 V (*a*); +2.5 V (*b*); +2 V (*c*); +1.5 V (*d*); +1 V (*e*); –2.5 V (*f*); –2 V (*g*); +2 V (*h*). Tunneling current: 0.3 nA. Below the images are the cross-sections taken along the correspondingly designated dashed lines. Cross-sections *c1* and *h1* were taken along essentially identical locations on the surface

prisingly, a repeated imaging (Fig. 3, *h*) at the same +2 V voltage as before (Fig. 3, *c*) does not produce an identical image. This is vividly demonstrated by cross-sections *c1* and *h1*, which are taken along physically identical locations on the surface. Therefore, our voltage-dependent STM results provide a hint that bright objects' shape and placement in Figs. 3, *b*–*h* are not specific to every particular sample bias voltage (in other words to the range of electron energies involved in the tunneling), but rather reflects the dynamic nature of the observed 2D overlayer interface at 300 K.

Comparing Figs. 3, *c* and 3, *h* reveals also the stability of the atomic lattice, which appears between the dynamically changing superlattice brightness maxima and is strongly reminiscent of the Ge(111)-2×2. Such images lead us to a tentative assumption about the reconstructed state of the germanium substrate below the 2D overlayer. In fact, this could be a Ge(111)-2 × 2, albeit rather defective, and with no long-range order, as it is actually the case on the uncovered areas of the substrate in Fig. 2, *b*. The reason for the invisibility of the 2 × 2 domains at higher bias voltages (Fig. 3, *a*) and their exposure at lower bias voltages (Figs. 3, *b*–*d*, *h*) could be a transparency of the overlayer for the tunneling electrons in the corresponding locations. Namely, the height/brightness minima of the superlattice may correspond to the parts of the overlayer, which do not possess (or have a very low density of) empty electronic states closer than 2.5 eV to the Fermi level of the sample. In this case, the tunneling of electrons from the tip proceeds directly into the substrate, which is then being imaged in such locations. Noteworthy, a similar "transparency" effect was observed by us for nm-scale 2-dimensional Bi islands on the Ge(111) substrate [17, 18]. However, one

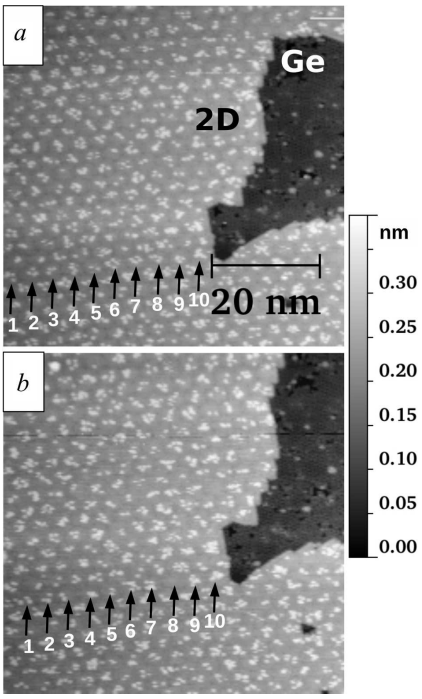

Fig. 4. Two consequtive STM images obtained on the same surface area (62 nm × 62 nm) of the Ge(111) sample showing an extended patch covered by the 2D overlayer. There is some small noticeable shift between the images due to the thermal drift and the STM piezoscanner creep). Sample bias voltage: –2.5 V, tunneling current: 0.3 nA. 10 identical superlattice sites are marked by numbered arrows on both images

should be careful in deducing the absence of electronic states in a certain energy interval (in other words, a band gap) from the fact of overlayer's transparency in STM. An alternative explanation could be some special form of overlayer's and tip's electronic wavefunctions, which may happen to produce a close-to-zero tunneling matrix element, thus eliminating the direct tunneling between the tip and the overlayer, even if the band gap is absent.

To further confirm the dynamics of the superlattice overlayer, we have also obtained two images in occupied states of the same area on the sample (Fig. 4) at the unchanging sample bias voltage (–2.5 V). The images in panels 4, *a* and 4, *b* were obtained one after another, and the field of view is slightly shifted due to the unavoidable thermal drift and the piezocreep in our experimental setup. However, the geometric configuration of the border between pure Ge and the 2D overlayer covered areas allows the unambiguous identification of each particular superlattice site in both panels (10 of such sequential sites are marked by numbered arrows for reader's convenience). Similar to the corresponding data in Fig. 3, we also observe various bright objects of atomic size. A detailed inspection of panels 4, *a* and 4, *b* shows no similarity in their number and configuration, in particular, some sites (see No. 8 among the marked ones) appear with or completely without bright objects in different images. It is worth mentioning that, despite obvious differences, some similarity of bright objects was still noticeable between consecutive images of Fig. 3. This can be explained by substantially different time intervals elapsed between the sequential imaging of identical superlattice sites in situations of Figs. 3 and 4 (roughly 1 min and 10 min, correspondingly), resulting from a larger field of view in Fig. 4 (62 nm × 62 nm) than in Fig. 3 (25 nm × 25 nm). This leads, in turn, to different acquisition times per single image. Therefore, given some dynamic processes constantly taking place on the sample, which are manifested by the constantly changing configuration of small bright objects, there is a less similarity of STM images for longer time intervals between two consecutive observations.

As was already pointed out, the STM images of the 2D superlattice show significant dependence on the probe tip condition. This is further demonstrated by Fig. 5, where different panels contain the same area with partial coverage by the 2D overlayer at different sample bias voltages in empty states. At +3 V in panel 5, *a*, the overlayer is imaged qualitatively similarly to the previous case at the identical tunneling bias in Fig. 3, *a*, showing the corrugated overlayer in the form of a hexagonal array with ca. 3.8 nm periodicity. However, at +2.5 V (Fig. 5, *b*), we observe small ripples superimposed on the principal corrugation, which become dominant at +2 V in Fig. 5, *c*. At +1 V in panel 5, *d*, as the tip gets closer to the surface, the resolution attained on the Ge(111) reconstructed areas is obviously better than in panels 5, *a*–*c* (all Ge atoms of the topmost layer, so-called adatoms, are clearly resolved), but the scanning above the 2D area becomes rather unstable due to the tip scratching against the surface. The onset of the scratching at around +1 V bias was also the case for the tip condition in Fig. 3, *e*. This behavior may originate from the scarcity of empty states close to the Fermi level within the 2D overlayer on the top of the *p*-type Ge(111) sub-

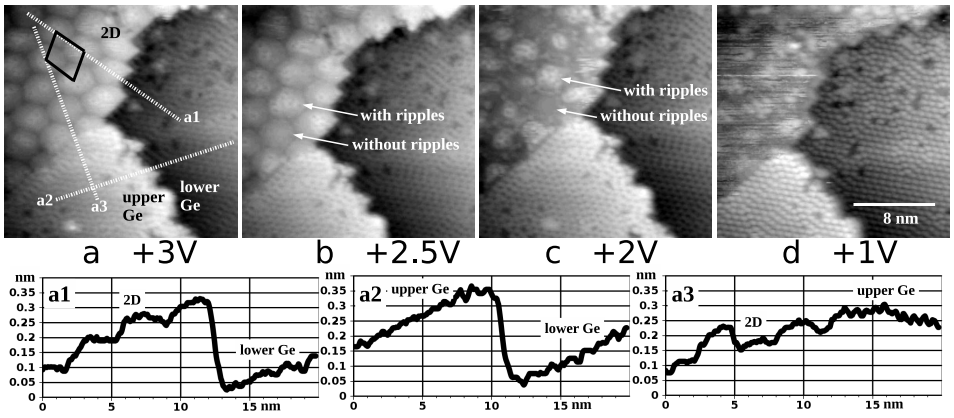

Fig. 5. STM images of the Ge(111) sample with two (upper and lower) neighboring terraces. The lower terrace is partially covered by the 2D overlayer adjacent to a single atomic step. All images are 25 nm × 25 nm in size and show the same area on the sample except for some shifts due to the thermal drift and the STM piezoscanner creep. Sample bias voltages are given directly below every panel. Tunneling current: 0.3 nA. Below the images are the height-distance cross-sections taken along the fine dashed lines in panel *a*

strate or alternatively to the poor coupling of their corresponding wave functions with those of the Pt-Ir probe tip.

The STM images in panels 5, *b* and 5, *c* are qualitatively different from their counterparts shown earlier in panels 3, *b* and 3, *c*, since no bright objects and no lattice on the atomic scale appear in the present case. Nevertheless, the ripples observed in panels 5, *b* and 5, *c* and also barely visible in panel 5, *a* are most probably of the same nature as the small bright objects in Fig. 3, due to their irregularity and the absence around certain superlattice sites (two neighboring sites with and without ripples are designated). Different types of images (Fig. 3 vs Fig. 5) at identical sample bias voltages could be a result of different probe tip's apex configurations. The latter is a well-known recognized uncertainty in every STM measurement, which is beyond the experimentalist's control.

The imaged area of Fig. 5 contains two neighboring germanium terraces separated by a single atomic step, while the lower terrace is partially covered by the 2D superlattice. The latter is immediately adjacent to the step in the lower left quarter of the imaged area, thus forming the "one-level" border between the overlayer and the reconstructed Ge(111). We can compare three kinds of boundaries by examining the corresponding cross-sections in panel 5, *a*: between areas on the same Ge terrace, which are covered and not covered by 2D (*a1*), a single atomic step on the Ge(111) substrate (*a2*), and finally between 2D on the lower terrace and pure Ge of the upper terrace (*a3*).

The cross-section *a1* confirms the ca. 0.3-nm height of the superlattice overlayer above the underlying germanium terrace, which was already deduced from the data of Fig. 2, *b*. It appears slightly lower than the regular 0.33-nm single atomic step on Ge(111), which is presented on cross-section *a2* for reference purposes. Likewise, the hexagonal superlattice periodicity of ca. 3.8 nm and the corrugation magnitude below 0.1 nm confirm the values obtained from similar cross-sections in Figs. 2 and 3. The height difference between the 2D overlayer and pure Ge across the "one-level" border in cross-section *a3* is below 0.05 nm, which agrees well with the step-heights in cross-sections *a1* and *a2*.

The parts of all three cross-sections in Fig. 5 marked as "lower Ge" and "upper Ge" are essentially contours of the atomically flat germanium surface, their small corrugation originating from the "adatoms" of the c(2 × 8), c(2 × 4), and 2 × 2 reconstructions of the Ge(111) surface. These adatoms are poorly resolved at high bias voltages in Fig. 5, *a*, but their resolution improves, as the bias voltage is lowered, when going from panel 5, *a* to panel 5, *d*. This allows us to define the crystallographic orientation of the substrate. Thus, cross-section *a3* coincides with the in-plane unit vector of Ge(111). The superlattice unit cell outlined in black in panel 5, *a* demonstrates the 30°-rotation between the unit vectors of the su-

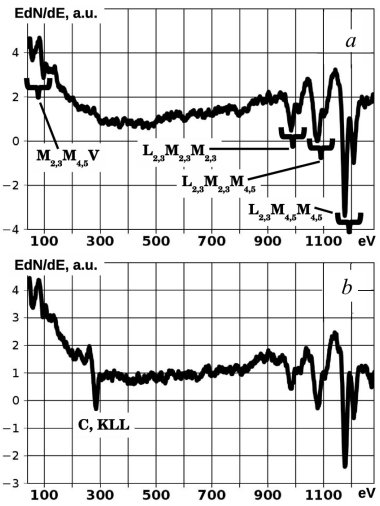

Fig. 6. Auger electron spectra of the Ge(111) substrate under clean (*a*) and carbon-contaminated (*b*) conditions. The EdN/dE spectra were obtained in the analog differentiation mode. The peaks in the spectra are designated according to their respective Auger transitions, which were excited by 3-keV primary electrons

perlattice overlayer and those of the Ge(111), in full agreement with the similar observation in Fig. 2, *b*.

5. Discussion

The results presented above summarize the observations of some new 2D (height corrugation in STM below 0.1 nm) surface structure, with a hexagonal in-plane periodicity of 3.8 nm and primitive translation vectors rotated by 30° relative to primitive translation vectors of the hosting Ge(111) substrate. This is drastically different from the previously known c(2 × 8), c(2 × 4), and 2 × 2 reconstructions of this semiconductor surface, rising immediately the question about the presence of some impurities. Carbon was the only impurity introduced onto sample's surface from the residual atmosphere of our vacuum chamber. This is demonstrated by the AES spectra in Fig. 6, where a spectrum of atomically clean Ge(111) is given in panel *a*, as compared to a strongly contaminated sample in panel *b*. Only Ge-originated multiplet peaks could be identified in the spectrum of Fig. 6, *a*, which are designated according to their respective Auger transitions: $M_{2.3}M_{4.5}V$, $L_{2.3}M_{2.3}M_{2.3}$, $L_{2.3}M_{2.3}M_{4.5}$, and $L_{2.3}M_{4.5}M_{4.5}$. If the sample was held for a sufficiently long time in the UHV environment of our vacuum chamber, we could detect the KLL Auger peak of carbon, as clearly seen in Fig. 6, *b*. No other chemical elements except germanium and carbon could be identified in this case, which means that carbon is, indeed, the only surface contaminant in our experimental setup.

The exposure to the UHV environment needed to obtain the 2D overlayer patches (Figs. 1, *b* and 2, *b*) was one order of magnitude shorter than that required to obtain the level of carbon contamination as in Fig. 6, *b*. The Auger spectrum obtained from the sample in Figs. 1, *b* and 2, *b* was similar to the one presented in Fig. 6, *a*. Since the intake of carbon is proven by the data of Fig. 6, *b*, we conclude that carbon is also present on the surface in Figs. 1, *b* and 2, *b*, but its quantity is too small to produce a signal above the noise level in our measurement. This correlates with the scarcity of the 2D overlayer patches, which could be found only after the extensive sampling by STM of randomly selected areas on our Ge(111) substrate. Also, the 900-K preparation temperature of our sample would be consistent with the possibility of carbon species to diffuse on the surface in order to be gathered in scarcely present patches far away from each other.

The observed 2D overlayer is of one-atom thickness (as proven by ca. 0.3-nm height above the underlying germanium substrate) and essentially atomically flat, since its corrugation of up to 0.1 nm is well below a typical single atomic step height. The later circumstance justifies the designation of such overlayer as two-dimensional. Assuming that the 2D overlayer patches are composed of carbon, the above-named characteristics are a strong hint that such overlayer is graphene (designated as g-C). The graphene formation is known to proceed at elevated temperatures from various carbon sources on metal substrates, which could be various hydrocarbon molecules arriving on the surface from the gas phase and undergoing a process of pyrolysis with hydrogen release, as reviewed in [3]. Another alternative is the segregation of carbon atoms to the surface from metal's bulk (if present there). Since the Ge(111) wafers used in our experiments were of high (microelectronics grade) purity, we can assume that the g-C was formed by the pyrolysis of hydrocarbon molecules, which are normally present in the residual atmosphere of the UHV chamber.

Although the presumed g-C layer is atomically flat, it is not absolutely flat. Its subatomic corrugation

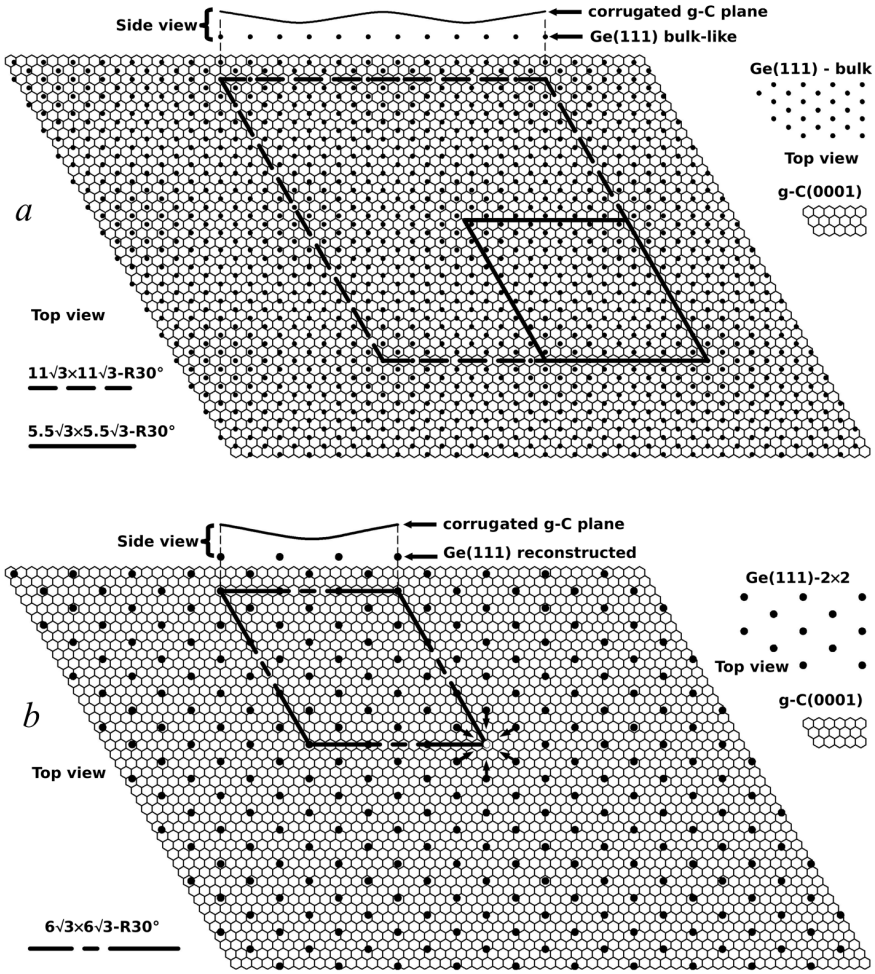

Fig. 7. Top and side views of the g-C(0001) lattice superimposed over the Ge(111) substrate in different states: *a*) unreconstructed bulk-like Ge(111); *b*) Ge(111)-2 × 2. In both cases, only the topmost layer of Ge atoms is shown: small black filled circles are Ge atoms in bulk-like positions (*a*); large black filled circles are topmost Ge adatoms of the 2 × 2 reconstruction (*b*). The g-C(0001) lattice is depicted as a set of hexagons, in which every corner designates the center of a C atom. The $5.5\sqrt{3} \times 5.5\sqrt{3} - R30°$, $6\sqrt{3} \times 6\sqrt{3} - R30°$, and $11\sqrt{3} \times 11\sqrt{3} - R30°$ supercells are designated by solid, dash-dotted, and dashed lines, correspondingly. Small black arrows in *b*) mark additional equilibrium positions, which become available for the neighboring adatoms, if a single adatom marked by an empty circle would be absent. The side views show qualitative height profiles of the graphene plane above the topmost Ge atoms along superstructure's unit cell in both panels

magnitude up to 0.1 nm and hexagonal lateral periodicity of ca. 3.8 nm, which is one order of magnitude higher than typical in-plane interatomic separations, are strongly reminiscent of the g-C on the top of a metal substrate in the case of a large lattice mismatch and a strong interaction in the film-substrate system (e.g., g-C/Ru(0001) [23–26]). In this case, the vertical corrugation arises due to the spatially alternating strong/weak film-substrate binding according to the coincidence lattice pattern between g-C(0001) and Ru(0001). In the case of the g-C/Ge(111) interface, we have two periodic structures: bulk-like unreconstructed Ge(111) of the 0.4-nm in-plane periodicity and g-C(0001) of the 0.246-nm in-plane periodicity. In Fig. 7, *a*, we show these two lattices superimposed on each other, where the Ge atoms are depicted by small filled black circles, while the C atoms are in the corners of the hexagons constituting the graphene plane. According to the observation of Fig. 2, *b* and Fig. 5, the superlattice observed on the g-C overlayers

is 30°-rotated relative to the Ge(111), which dictates the g-C(0001) primitive unit vectors to be 30°-rotated relative to those of the Ge(111).

The model in Fig. 7, *a* demonstrates the laterally periodic alternating atomic geometry at the interface between g-C(0001) and bulk-like Ge(111). If a C atom is placed directly above the Ge atom at some location, than, due to the lattice mismatch, such situation can not be realized everywhere at the surface. Namely, other geometries will also be realized: a center of the g-C lattice hexagon is above the substrate Ge atom, as well as all possible intermediate non-symmetric cases of mutual positioning of Ge and C atoms. All these situations will be regularly repeated with the periodicity of the coincidence lattice, which will be determined by laterally coinciding integer sets of substrate/overlayer unit cells.

If the Ge(111) and g-C(0001) planes are rotated by 30° with respect to each other, than the Ge atoms appear with the 0.693-nm periodicity ($R30°$ unit) along the primitive translation vector ([1000] direction) of g-C. An extremely good match exists between 11 $R30°$ units of Ge(111) and 31 primitive units of g-C(0001): $11 \times 0.693 = 7.623$ and $31 \times 0.246 = 7.626$ (if rounded to a third digit). The length of the $R30°$ unit is $\sqrt{3}$ of that of the primitive Ge(111) unit. Therefore, the above-described match would lead to the g-C/Ge(111) $11\sqrt{3} \times 11\sqrt{3} - R30°$ overlayer structure. Its lateral periodicity is 7.6 nm, which is $11\sqrt{3}$ times larger than the 0.4-nm primitive in-plane translation vector of the bulk-like Ge(111). The 7.6-nm superlattice period doesn't stand in line with the 3.8-nm value observed in our STM images. This discrepancy is easily resolved by a trivial arithmetic examination of other matches between various numbers of substrate's and overlayer's unit cells. In particular, a fairly good match is discovered for 5 or 6 R30° substrate units: $5 \times 0.693 = 3.465$ and $14 \times 0.246 = 3.444$, or $6 \times 0.693 = 4.158$ and $17 \times 0.246 = 4.182$. This means that although it takes the 7.623-nm lateral distance for the atomic geometry to be repeated extremely precisely on the g-C/Ge(111) interface, it will also be repeated to a fair extent only half-way to the completion of the $11\sqrt{3}$ period. Indeed, a detailed examination of Fig. 7, *a* reveals that the g-C "honeycombs" can be found centered on the Ge substrate atoms not only at the corners of the $11\sqrt{3} \times 11\sqrt{3} - R30°$ supercell, but also in its central part and around the middle of its every side. Therefore, the resulting superlattice is described by the $5.5\sqrt{3} \times 5.5\sqrt{3} - R30°$ unit cell (solid line in Fig. 7, *a*) and will have a periodicity of 3.811 nm, which is in excellent agreement with the superlattice observed by STM in the present work and is a decisive argument in favor of the positive graphene identification!

Although we do not resolve the graphene atomic lattice, we deduce its periodicity from the known lattice parameters of the substrate and the observed parameters (orientation and periodicity) of the g-C overlayer's corrugation. Conceptually, it is similar to solving an equation (unknown lattice) + + (known lattice) = (superlattice) with one unknown constituent. The interfacial structure suggested in Fig. 7, *a* is a film/substrate system with a tremendous lattice mismatch: the primitive in-plane translation vectors are 0.4 nm for Ge(111) and 0.246 nm for g-C(0001). Such mismatch usually prevents the heteroepitaxial film growth in a layer-by-layer mode. However, in the case of graphene acting as a film-building substance, such growth can be realized due to the extreme strength of this 2D material. If the interfacial strain energy is not high enough to tear the g-C sheet apart, it will grow on the substrate retaining its in-plane integrity.

Exploiting the analogy with various metal substrates [3,9], one can assume that the strongest bonding between graphene and germanium is achieved, when the C atom is placed directly above the substrate atom, while the weakest bonding is realized when the center of the g-C hexagon is directly above the Ge atom. Such exact binding assignment is only a tentative assumption, which will have to be confirmed by *ab initio* calculations, but the laterally periodic changes of the interfacial atomic geometry should inevitably lead to corresponding variations of the binding strength. In fact, any particular kind of the atomic geometry assignment to the corresponding binding strength will lead to a g-C overlayer corrugation (modulation of its height), as observed in STM and depicted qualitatively by the atomic model's side view on the top of Fig. 7, *a*. This is guaranteed by the laterally periodic changes of interfacial geometry due to mismatched lattices of the film and the substrate. We believe that such situation is indeed observed by STM at high positive sample bias voltage in Figs. 1, *b*, 2, *b*, 3, *a* and 5, *a*.

The real interfacial structure may be actually more complicated than depicted by Fig. 7, *a*, where the

overlayer is placed on the bulk-terminated Ge(111). The tendency of the semiconductor surfaces to reconstruct is a well-known fact, but this relates to semiconductor/vacuum interface, while the issue of semiconductor/2D material is yet to be clarified. The STM images in Figs. 3, *b–d, h* are strongly suggestive about seeing the Ge(111) substrate in the reconstructed state under the g-C overlayer. Such suggestion is based on the g-C overlayer's transparency for the tunneling electrons, which is so far only speculative and must be confirmed by *ab initio* electronic structure calculations of the g-C/Ge(111) system. In Fig. 7, *b*, we consider the case of g-C placed on the Ge(111)-2×2, since exactly this simplest type of the reconstruction is supposedly imaged by STM through the transparent sections of the graphene film. Apart from the bulk-like termination of Ge(111), its reconstructed state includes two additional atomic layers: the layer with the so-called restatoms and backbond atoms and the topmost layer containing the so-called adatoms, as exhaustively discussed in the literature [16, 19–22]. To avoid clutter, only the adatoms are depicted in Fig. 7, *b* as large filled circles, the depiction of the graphene layer is the same as in Fig. 7, *a*.

On the reconstructed Ge(111)-2×2 surface, adatoms' positions are directly above the atoms of the bulk-terminated layer, but the periodicity of their placement (0.8 nm) is twice that within the bulk-like Ge(111). Therefore, in Fig. 7, *b*, the Ge atoms below the g-C layer are placed twice as rarely than in Fig. 7, *a* along any in-plane direction. This removes the possibility to match any odd number of $R30°$ substrate units of Ge(111) with the graphene lattice. The only satisfactory match with a realistic periodicity is the $6 \times 0.693 = 4.158$ vs $17 \times 0.246 = 4.182$, which was already discussed in the context of Fig. 7, *a*. This match would produce a $6\sqrt{3} \times 6\sqrt{3} - R30°$ superstructure, its unit cell being marked in Fig. 7, *b* by a dot-dashed line. However, its ca. 4.2-nm periodicity is substantially higher than the experimentally observed value, so such construction cannot describe the real g-C/Ge(111) interface.

In the meantime, the real 2×2 reconstruction is never observed in such perfect state, as drawn in Fig. 7, *b*. As usual, it is highly defective (including numerous adatom vacancies), lacks any long-range order, and consists of small incoherent domains. The STM images in Figs. 2 and 5 illustrate this situation rather vividely. In the ideal 2×2 superstructure, the adatoms cannot shift laterally from their positions, being held in place by the available low-energy coordination from the lower atomic layer (not shown in Fig. 7, *b*). This "stability" changes if at least one adatom is absent, i.e., when an adatom vacancy is present, a kind of a situation encountered very often on the real surface. For instance, if one of the adatoms, which is designated by the open circle in Fig. 7, *b*, is absent, then any of the neighboring adatoms can occupy not only this given vacancy, but also any of the locations at the ends of the small black arrows. Any of such motions, in turn, will open up further possibilities for other adatoms farther away from the initial vacancy to move into alternative local energetic minima sites, and so on. This scenario results in a situation where the graphene overlayer is supported by a stochastic mixture of small c(2×8), c(2×4), and 2×2 domains similar to the bare Ge areas in Figs. 2, *b* and 5.

If the substrate is indeed a mixture of domains of the type described above, then various adatoms may occupy positions in or not in registry with the initial "ideal" (long-range ordered) 2×2 superlattice, but in any case they will always remain in registry with the unreconstructed Ge(111) depicted in panel 7, *a*. The latter fact is derived from the geometry of various reconstructed phases of Ge(111), as already comprehensively discussed in the literature [16, 19–22]. The actual interfacial structure can be obtained from Fig. 7, *a* by a random removal of three quarters of Ge atoms under the condition that the remaining Ge atoms are at least 0.8 nm apart. Thus, the remaining Ge atoms will retain the registry of the bulk-like Ge(111) plane, and the coincidence lattice with the smallest periodicity will be again $5.5\sqrt{3} \times 5.5\sqrt{3} - R30°$, identical to that in Fig. 7, *a*. Its periodicity of 3.811 nm is $5.5\sqrt{3}$ times larger than the 0.4-nm primitive in-plane translation vector of the bulk-like Ge(111).

Placing graphene on the domain-rich reconstructed Ge(111) substrate with no long-range order and with some adatom vacancies can also explain the dynamic behavior observed in Figs. 3 and 4. As already discussed above for a single adatom vacancy in Fig. 7, *b*, its presence leads to a possibility of a chain of adatom jumps with virtually unlimited number of resulting adatom geometries. Such jumps are not unusual on a reconstructed Ge(111) at 300 K and were already

reported in the literature [16, 27]. We can tentatively suggest that such jumps can also take place under the g-C layer, while the latter may in fact facilitate them by lowering the energy barrier for adatoms to move between the neighboring low-energy sites (sitting on such a site, the adatom saturates the chemical bonds with three atoms of the lower layer, so-called back-bond atoms). We speculate that the resulting different atomic geometries of the substrate may lead to strong local modifications of g-C overlayer's electronic structure manifested as the bright objects superimposed on the smooth superlattice height corrugation, as observed in Figs. 3, 4. Needless to say, this interpretation will have to be confirmed by *ab initio* electronic structure calculations and the simulation of corresponding STM images.

It is worth noting that the preliminary STM observations of a similar g-C/Ge(111) superlattice were previously reported by us [26]. The STM measurements performed in that work were not precisely calibrated, which led to a conclusion about the g-C/Ge(111)-8 × 8 superlattice. Indeed, a very good match exists between 8 in-plane units of Ge(111) and 13 g-C(0001) units: $8 \times 0.4 = 3.2$ vs $13 \times 0.246 = 3.198$, if the directions of primitive translation vectors of Ge(111) and g-C(0001) coincide with each other. Such conclusion was reached on the basis of a sole observation of the g-C/Ge(111) superlattice without any reference to substrate's crystalline orientation. In the meantime, the precise measuring of the periodicity by means of STM is complicated by a number of factors. The thermal drift of a mechanical set-up and the creep of piezoactuators in the STM scanner produce uncontrollable motions of the probe tip relative to the investigated sample. The calibration of the piezoactuators is subjected to changes due to the material aging. As a result, substantial geometrical distortions are introduced into the obtained STM images, hindering the precise measurement of distances. An additional complicating factor in the case of the g-C/Ge(111) interface is the stochastic nature of the configuration of brightness maxima, as systematically revealed in the present work. This introduces a further uncertainty into the determination of the superlattice periodicity. The observations reported in [26] were of preliminary approximate character, without taking all these circumstances into account. They suggested a structure with a periodicity close to 3.2 nm, so the obvious 8:13 matching combination was selected for a tentative interpretation of the coincidence lattice.

Our present work includes a systematic study of the g-C/Ge(111) superlattice alongside with uncovered Ge(111) areas within a single STM image. This has allowed us to exclude the thermal drift, creep, and calibration issues, due to the immediate presence of the reference in the form of the reconstructed domains of pure Ge(111), for which the interatomic distances are established and well known. This allowed us to reveal the orientation of the g-C/Ge(111) superlattie relative to the atomic registry of Ge(111), which was not available in the previous work. Thus, our present precise observation yields such superlattice parameters as the 3.8-nm periodicity with translation vectors rotated by 30° relative to the primitive ones of Ge(111). As these parameters are established, they strongly hint on the g-C/Ge(111) $5.5\sqrt{3} \times 5.5\sqrt{3} - R30°$ interfacial superstructure.

6. Conclusions

We have presented a UHV STM investigation of the unusual long-period 2D surface superstructure on the Ge(111) substrate, which is drastically different from its any known reconstructions. This superstructure is a 3.8-nm periodic hexagonal lattice of corrugation with subatomic magnitude, which is the $5.5\sqrt{3} \times 5.5\sqrt{3} - R30°$ superstructure relative to the bulk-like termination of Ge(111). Based on the knowledge that carbon is the only contaminant on the sample in our UHV system, we suggest that the observed 2D superstructure is the graphene overlayer, which is corrugated according to the lateral periodicity of the coincidence lattice between the Ge(111) and g-C(0001) atomic planes. The topmost Ge adatoms can change their placement among a great number of localy available equilibrium positions already at 300 K, producing drastic changes in the local electronic structure, as observed by STM in real time at various sample bias voltages. Our model is a purely intuitive interpretation of the available experimental data and must be confirmed by future *ab initio* calculations of the equilibrium atomic geometry of the g-C/Ge(111) interface and the corresponding electronic structure. Further experiments are required to prove the presence of graphene in a decisive manner by means of Raman spectroscopy, as well as submonolayer amounts of carbon contamination by various electron spectroscopy techniques.

All processing of STM data was performed using the Gwyddion software package, which is available as an "open source" and can be downloaded from the gwyddion.net website. We are thankful to Dr. I. Lyubinetsky for generously providing the Ge(111) wafers.

1. K.S. Novoselov, A.K. Geim, S.V. Morozov *et al.*, Science **306**, 666 (2004).
2. A.H. Castro Neto, F. Guinea, N.M.R. Peres *et al.*, Rev. Mod. Phys. **81**, 109 (2009).
3. J. Wintterlin and M.-L. Bocquet, Surf. Sci. **603**, 1841 (2009).
4. U. Starke and C. Riedl, J. of Phys.: Cond. Matt. **21**, 134016 (2009).
5. S. Akcöltekin, M.El. Kharrazi, B. Köhler *et al.*, Nanotechn. **20**, 155601 (2009).
6. P. Blake, E.W. Hill, A.H. Castro Neto *et al.*, Appl. Phys. Lett. **91**, 063124 (2007).
7. A.K. Geim and K.S. Novoselov, Nature Mater. **6**, 183 (2007).
8. L. Simon, M Stoffel, P. Sonnet *et al.*, Phys. Rev. B **64**, 035306 (2001).
9. C. Oshima and A. Nagashima, J. of Phys.: Cond. Matt. **9**, 1 (1997).
10. A. Banerjee and H. Grebel, Nanotechn. **19**, 365303 (2008).
11. R.W. Olesinski and G.J. Abbaschian, Bull. Alloy Phase Diagr. **5**, 484 (1984).
12. H.E. Elsayed-Ali and X. Zeng, Surf. Sci. **538**, 23 (2003).
13. G. Wang, M. Zhang, Y. Zhu *et al.*, Sci. Reports **3**, 2465 (2013).
14. I.V. Lyubinetsky, P.V. Melnik, N.G. Nakhodkin *et al.*, Vacuum **46**, 219 (1995).
15. I.V. Lyubinetsky, Ukr. J. Phys. **60**, 160 (2015).
16. A. Goriachko, P.V. Melnik, M.G. Nakhodkin, Ukr. J. Phys. **60**, 1132 (2015).
17. A. Goriachko, P.V. Melnik, A. Shchyrba *et al.*, Surf. Sci. **605**, 1771 (2011).
18. A. Goriachko, A. Shchyrba, P.V. Melnik *et al.*, Ukr. J. Phys. **59**, 805 (2014).
19. R.S. Becker, B.S. Swartzentruber, J.S. Vickers *et al.*, Phys. Rev. B **39**, 1633 (1989).
20. E.S. Hirschorn, D.S. Lin, F.M. Leibsle *et al.*, Phys. Rev. B **44**, 1403 (1991).
21. G. Lee, H. Mai, I. Chizhov *et al.*, J. of Vac. Sci. and Techn. A **16**, 1006 (1998).
22. G. Lee, H. Mai, I. Chizhov *et al.*, Surf. Sci. **463**, 55 (2000).
23. S. Marchini, S. Günther, J. Wintterlin, Phys. Rev. B **76**, 075429 (2007).
24. A. Goriachko, H. Over, Zeit. Phys. Chem. **223**, 157 (2009).
25. B. Borca, S. Barja, M. Garnica *et al.*, Semicond. Sci. Techn. **25**, 034001 (2010).
26. A. Goriachko, P.V. Melnik, M.G. Nakhodkin *et al.*, Materialwiss. Werkstofftech. **44**, 129 (2013).
27. A.J. Mayne, F. Rose, C. Bolis *et al.*, Surf. Sci. **486**, 226 (2001).

Received 13.05.15

А. Горячко, П.В. Мельник, М.Г. Находкін

ПРОПОЗИЦІЯ СТРУКТУРИ
ГРАФЕН/Ge(111) НА ОСНОВІ ДОСЛІДЖЕННЯ
МЕТОДОМ СКАНУЮЧОЇ ТУНЕЛЬНОЇ
МІКРОСКОПІЇ У НАДВИСОКОМУ ВАКУУМІ

Р е з ю м е

У роботі наведено результати експериментальних спостережень методом скануючої тунельної мікроскопії нової поверхневої надструктури $5,5\sqrt{3}\times 5,5\sqrt{3}-R30^\circ$ на підкладці Ge(111). Їй притаманні яскраво виражені ефекти локальної густини електронних станів, що спричиняють сильну залежність СТМ зображень від тунельної напруги, а також їхні динамічні зміни при 300 K. Запропоновано інтерпретацію даної надструктури як графену, що формується у малих субмоношарових кількостях шляхом піролізу вуглеводневих складових залишкової атмосфери вакуумної камери під час відпалу зразка Ge(111) при 900 K. Побудовано атомарну модель гетероепітаксійного інтерфейсу графен/Ge(111)-$5,5\sqrt{3}\times 5,5\sqrt{3}-R30^\circ$, що відзначається реконструйованою підкладкою Ge(111) без дальнього порядку під шаром графену, який є періодично вигнутим по висоті внаслідок просторових варіацій міжатомної геометрії надзвичайно сильно неузгоджених ґраток Ge(111) та графен(0001).